X-692-74-49
PREPRINT

A DISCUSSION OF INTERPLANETARY POST-SHOCK FLOWS WITH TWO EXAMPLES

KEITH W. OGILVIE
LEONARD F. BURLAGA

JANUARY 1974

GSFC
GODDARD SPACE FLIGHT CENTER
GREENBELT, MARYLAND

For information concerning availability of this document contact:

Technical Information Division, Code 250
Goddard Space Flight Center
Greenbelt, Maryland 20771

(Telephone 301-982-4488)

A DISCUSSION OF INTERPLANETARY POST-SHOCK FOLWS WITH TWO EXAMPLES

K. W. Ogilvie
L. F. Burlaga

Laboratory for Extraterrestrial Physics
NASA/Goddard Space Flight Center
Greenbelt, Maryland 20771

Short Title: Interplanetary Post-Shock Flows

Abstract

The paper describes plasma and magnetometer observations of two flare-associated shock flows and the comparison of them with present models. One represents a class of flows where the shock is followed by a stream and separated from it by a region in which density temperature and speed decrease monotonically. Neither the blast wave model or the 2-stage model in which the stream and shock are attributed to the same flare can quantitatively describe this class. The other is characterized by a complex region between the shock and the following stream, which has many discontinuities and fluctuations, but in which there is no increase in Helium concentration. This class of event is not describable in terms of the conventional pictures presented, for examply by Hundhausen. These two types of flow can be distinguished using ground magnetograms, since the former shows no sudden impulses following the shock whereas the latter shows many.

We suggest that the complexity of post shock flows is often due to the interaction of the shock with streams having different origins from the shock. A stream which is observed to follow a shock by ~1 day either has a different source from the shock or its acceleration is not described by the accepted solar wind expansion models.

I. Introduction

Several theories and models of post-shock flows in the solar wind have been proposed, and were recently reviewed in detail. (Korobeinikov and Nikolayev, 1972; Hundhausen, 1972; Dryer, 1972; and Burlaga, 1972). They can be briefly described as follows:

1) An instantaneous energy input at the sun produces a blast wave (Parker 1963), which is detected as a fast shock followed by monotonically decreasing plasma density, bulk speed and temperature.

2) A step-function energy input at the sun produces a driven shock wave. Density, bulk speed, and temperature rise behind the shock and subsequently decrease.

3) Intermediate cases, due to energy increases lasting several hours, and producing flows with profiles intermediate between 1 and 2 above.

4) Hundhausen et al. 1970 and Hundhausen, 1972 introduced a 2-stage model. Unlike the previous three types of shock flows, which are found by solving hydrodynamic equations, this is a conceptual model intended to explain certain observed events characterized by a shock followed for several hours by a blast wave-like profile which is followed in turn by a stream within 24 hours. According to this model, the shock is a blast wave produced by a flare explosion, and the stream is the result of heat generated by the flare and retained near the flare site.

5) Synoptic model. This is a continually changing model based on a

conceptual synthesis of various types of observations. The current model is described by Hundhausen (1972) and Burlaga (1972). It describes the post shock flow by the following series of events: shocked interplanetary gas, a tangential discontinuity, enhanced $^4He^{++}/H^+$ ratio, and a magnetic bottle within which the proton and electron temperatures are depressed as a result of expansion.

Shock waves have also been classified by Hundhausen (1970) on the basis of observations as F events and R events, corresponding to a fall or rise, respectively, of $nU^3/2$ behind the shock front, and as M events and F events corresponding to corotating and non-corotating shocks, respectively, by Colburn and Sonett, 1968.

In the course of analyzing two shock waves observed in 1971 by Explorer 43, we found none of the above theories and models were able to describe these events satisfactorily. After discussing our evidence, we suggest another model, the compound event model, based on the idea that the observed flow behind a shock front is not necessarily directly related to the shock wave and that a shock and a stream behind it might have different origins. It is not suggested that this model applies to all shock waves, but it does describe some events in the literature better than the current models.

To put into perspective the two shock waves to be discussed, we show in Figure 1 a plot of the sum of magnetic and thermal energy densities,

$$\left[\underline{P} = B^2 / (8\pi) + n_p kT_p + n_e kT_e + n_\alpha kT_\alpha\right]$$

for the period March 18 to April 8, 1971; here B is from the GSFC

magnetometer on Explorer 43, T_p and n_p are from the GSFC plasma analyzer on the same spacecraft, T_e is set equal to 1.5×10^5 °K (Scudder et al., 1973, Montogomery et al., 1968), and $T_\alpha = 4T_p$. (Hundhausen, 1972). Four distinct regions of enhanced P can be seen in Figure 1, corresponding to the "interaction regions" singled out by Burlaga and Ogilvie (1970) as regions in which major dynamical processes are occurring near 1 AU. This paper discusses only the events starting on March 19 and April 3, which begin with a very abrupt increase in P corresponding to the arrival of a shock front.

II. Instrument and Data Reduction Methods

Goddard Space Flight Center provided two plasma instruments, positioned 180° apart in the Explorer 43 spacecraft which rotates once every 11.1 seconds, about an axis maintained at 90° ± 1° to the ecliptic plane. The first instrument was a cylindrical electrostatic analyzer-secondary emission detector combination with a field of view 1° by ± 18°, with the larger angle in a plane containing the spin axis. The sun-ward semi-circle of rotation was divided into 11.25° sectors, and the 45° about the heliocentric direction was further divided into 2.8° sectors. The energy per charge range of this device was from 173 to 6068 eV/Z, in twenty differential intervals of width 3.2%, sampled sequentially, one each spin. The second instrument consisted of a cylindrical analyzer with sensitive angles of 1° in azimuth and ± 9° in a plane containing the spin axis, followed by a Wien filter tuned to pass only ions with a mass per charge of two. It has an energy range from 675 to 7625 eV

covered in twenty differential intervals of width 3%. Thus, the first instrument responded to all ions, while the second was sensitive mainly to $^4He^{++}$.

One purpose of the latter instrument was to provide an unambigous Helium distribution function which could be used to interpret the results of the more sensitive energy per charge instrument.

Fluid Parameters for the protons were obtained as follows. Counts from the energy per charge detector were accumulated for each spin, and the resulting twenty numbers, after subtraction of a small background, were fitted by means of a least-squares technique to the sum of two convected maxwellian velocity distributions, one for the protons of density n_p, temperature T, and bulk speed U, and the other for $^4He^{++}$ ions with density n_α, temperature 4T, and bulk speed U. This neglects temperature anisotropy, T falling between $T_{||}$ and $T_\perp$ for the protons, and assumes that helium has the same velocity as the protons. The low residuals usually obtained in the fitting process indicate that these assumptions are usually well obeyed.

Fluid parameters for the α particles were obtained from the He detector by correcting counts for background, fitting the spectrum with a spline, and taking appropriate moments. The proton parameters obtained by the least squares technique described above were checked using a similar technique given the α particle distribution function obtained as just described. The α particle contribution to the E/Z spectrum was subtracted to obtain a proton spectrum which was then fitted by a spline and integrated to obtain the moments. The two methods of computing pro-

ton densities and speeds normally give results which agree within a few percent.

The 3-axis fluxgate magnetometer carried by this spacecraft was provided by Dr. Ness of GSFC. The sampling frequency of this instrument is 12.5 measurements/sec, but for this study 5.6 sec averages were used, since the associated Nyquist Frequency then corresponds more closely to that of the plasma instrument.

III. The March 19, 1971, Shock

Shock front and its relation to sun. The abrupt increase in pressure, P, at Explorer 43 between 1141 and 1145 UT on March 19, 1971 (Figure 1) clearly indicates the passage of a nonequilibrium structure. Figure 2 shows that this increase in pressure is the result of simultaneous increases in n_p, T_p, and B, as one expects for a forward, fast magnetofluidynamic (MFD) shock. The same figure shows a simultaneous increase in U with respect to a fixed (spacecraft) frame, corresponding to a decrease in U with respect to a frame moving away from the sun with the shock, again consistent with such an interpretation. Thus, the discontinuity has the signature of a forward, fast MFD shock. In the framework of MFD, this signature uniquely identified the shock.

A quantitative discussion of the shock front would require knowledge of the shock normal. Since data from only one spacecraft are available, use must be made of the coplanarity theorem to compute $\underset{\sim}{n}$, e.g. $\underset{\sim}{n} \sim (\underset{\sim}{B}_2 - \underset{\sim}{B}_1) (\underset{\sim}{B}_2 \times \underset{\sim}{B}_1)$. Unfortunately, this method cannot be used unambiguously here because there is no single, clearly defined post-shock $\underset{\sim}{B}_2$. This is

illustrated in Figure 3, which shows the magnitude B and direction (θ,Φ) in the solar ecliptic coordinate system on scale of $\approx$ 5 min. The magnetic field direction changed by 12° in $\leq$0.8 min., coincident with a 2-fold increase in B between 1144.58 and 1145.09 but the field direction changed by a further 18° from 1145.09 UT to 1146.11 UT, with a correspondingly large ambiguity in B_2. We define σs and Φs as the solar ecliptic lattitude and azimuth of the coplanarity shock normal. Using values of B very close to the discontinuity, we obtain σ_s = 16°, Φ_s = 102°, whereas the procedure of Chao and Lepping (1973) which uses averages over several minutes gives σ_s = -52°, Φ_s = 147°. The ambiguity in the shock normal does not seriously affect the following discussion of the post-shock flow, which is based only on the identification of the discontinuity in question as a shock front and not on its detailed properties.

It is not possible to unambiguously associate this shock with a flare. Chao and Lepping (1973) make no flare assignment. However, the following evidence indicates that the shock is more likely to be flare associated than corotating.

A sudden ionospheric disturbance took place between 0655 and 0720 UT on March 17, associated with a flare of importance 1N, situated at (N20, W20) in region 11192 on the solar disc. According to Solar Geophysical Data (1971) there was a complex radio event of peak flux density 10^{-17} WM^{-2} Hz^{-1} at 0644 UT. A small x-ray event and solar protons in the 0.6 to 13 MeV energy range starting between 0100 and 1300 UT on March 17 were observed by the University of Chicago detector on Pioneer 6, located 45° heliocentric longitude west of the earth. The flare was thus associated with several effects in the interplanetary medium. No type II or type IV

radio bursts were reported, but they were probably not being monitored at this time (Sakurai, private communication). If we assume that the March 19 shock was caused by the March 17 flare, the transit time 53 hrs. giving an average speed of 780 km/sec. This speed is well within the range of the distribution of average speeds given by Chao and Lepping (1973), although somewhat greater than the most probable average speed.

The probability that the shock was corotating is small, since few corotating fast forward shocks have been observed despite deliberate searches for them (Ogilvie, 1972; Unti, Neugebauer and Wu, 1973). However, to consider this possibility, records of ssc's were examined for 27 day recurrences, on the assumption ssc's are caused by shocks. Ssc's were observed on January 27, February 23, March 19, and April 14, 1971, at intervals of 27, 24, and 26 days, respectively. The April 14 event was probably caused by a flare, (Chao and Lepping, 1973), so we are left with only two intervals. Since the intervals between the March 19 shock and that which preceded it is 24 days rather than 27 days it is difficult to argue that the shock was corotating on this basis. Finally, the observed post shock profile, to be discussed later, is not what one expects for a shock produced by a corotating stream.

In summary, the March 19 shock was probably not corotating, but it is likely to have been the result of a flare of importance 1N at (N20, W20) on 17 March, 1971.

Post Shock Flow. The post-shock profiles of the energy flux ($\frac{NU^3}{2}$), speed, density, temperature, magnetic field, and α particle to proton ratio are presented in Figure 2 for the March 19, 1971 event.

From the montonic decrease in $NU^3/2$ it would be classified as an F event in the notation of Hundhausen (1972).

The post-shock flow pattern in Figure 2 is clearly not that of a driven shock or an intermediate shock. It also differs greatly from that implied by the synoptic mode; there is no He^{++} enrichment, and no outstanding discontinuity.

The profile for the 13 hr. interval behind the shock resembles that of a blast wave. The energy <w> and mass <m> computed in the manner described by Hundhausen (1972) are 1.7×10^{31} ergs and 1.4×10^{16} gm, respectively, essentially identical to the average values for observed F-type waves given by Hundhausen (1972). The predicted transit time from 0.1 to 1.0 AU for such a blast wave, according to Hundhausen and Gentry (1969), is $\approx$ 51 hr., which compares favorable with the observed propagation time of 53 hour.

The speed profile is actually very similar to that of the October 5, 1967, event (Gosling et al., 1968; Hundhausen et al., 1970). Hundhausen et al. (1970) and Hundhausen (1972) suggested the 2-stage model to explain this profile, the shock being generated by a flare explosion and the stream being the result of heating subsequent to, but associated with the flare. However, the following argument indicates that in the March 19 event, the stream is probably not caused by the flare. (A similar argument applies to the Oct. 5 event, and gives the same conclusion.)

An upper limit limit for the transit time of a stream can be obtained using the radial profile of the solar wind speed given by

Parker's solution for an isothermal corona. In this case, $U(r) \propto r^{1/4}$ and the time for a volume element having speed Ue at 1AU to propagate from the sun to 1AU is $t_e = (4/3)(r_e/U_e)$ (Burlaga, 1967). With r_e = 1AU and U_e = 440 km/sec., the maximum speed of the stream, we find that t_e = 126 hours. The maximum flow speed occurred on March 20 at about 1100 UT, and assuming it to be accelerated as part of the solar wind, the corresponding plasma element must have left the sun on March 15 at about 0500 UT, approximately two days before the tentatively assigned flare. A lower limit for the transit time, obtained by assuming a constant solar wind speed of 440 km/sec., is $t_e \approx 100$ hours. This also implies that the stream was emitted before the occurrance of the flare. Thus, we conclude that the stream was probably not caused by the flare, and we must reject the 2-stage model for this event.

Having found that none of the standard models satisfactorily describes the observations, we now suggest a new model. The idea is simply that the stream and the shock might have entirely different origins. In particular, the calculation in the preceding paragraph suggests that the stream existed before the shock and that consequently the shock might have passed through the stream. For both the March 19 event and the October 5, 1965 event which has been associated with a 2^+ flare (Gosling et al., 1968), the flare was $\approx 20°$W of central meridian. Thus, the configuration for these two events is presumably that illustrated in the top of Figure 4. A stream was emanating from somewhat west of central meridian at the time of the flare. As the stream corotated, the shock moved outward, part of it passing through

the stream and arriving at the earth ahead of the stream. If the stream had originated farther to the west, the shock and stream might have arrived nearly simultaneously at the earth, as illustrated in Figure 4B. If the stream originated farther toward the east, the stream would be seen much later than the shock, as shown in Figure 4C, and the flow might even be complicated by other streams. This model, then is quantitatively consistent with the observed profiles for the October 5, 1965 and March 19, 1971, events, can account in part at least for the great variety of post-shock profiles noted by Ogilvie et al., (1968), and does not require assumptions about the ejection of material by the sun.

An interesting feature of this event is the absence of discontinuities and larger fluctuations between the shock front and stream, in contrast to the event to be described below. To distinguish these two type of flows, we refer to the March 19 event pattern in which there are no discontinuities in momentum flux and consequently no sudden impulses in the corresponding magnetograms, as a continuous flow, and the pattern described below as a discontinuous flow.

IV. April 3, 1971 Event

Shock front and relation to the sun. Figure 1 shows that the event began at $\approx$2125 UT on April 3 with an abrupt increase in pressure, P, signaling the arrival of a non-equilibrium structure. Figure 6 shows that the increase in P was due to a simultaneous increase in U, n_p, T_p, and B, the signature for a forward, fast, MFD shock. Higher time-

resolution magnetic field data reveal a very complex shock structure. It is not possible to calculate the normal using the coplanarity theorem, because there is no well-defined pre-shock state. The complexity and width of the field profile are unusual among these interplanetary shocks which have been studied.

This shock, observed by Explorer 43 at 2125 UT on April 3, was related to a flare of importance 3N which took place between 1350 and 1430 UT on April 1. This identification has also been made by Chao and Lepping (1973). There were 2 or more H_α maxima during this time, and the flare occurred in active region 11221 at (S20, W13). There was an x-ray event, and protons with energies >10 MeV were emitted (Bostrom-private communication). Assuming this identification, the mean propagation speed to 1 AU was 740 km sec.$^{-1}$ a typical shock speed. There is no evidence that this shock was corotating.

Post-Shock Flow. Figure 1 shows that the interaction region, i.e. the region of enhanced P, is located between the shock front and a stream beginning at $\approx$ 0200 UT on April 5, making it appear that the shock is driven by the stream. However, the energy flux does not have the behavior that one expects for a driven-shock, but neither decreases monotonically.

Note that although it is an F-type event, it is not a blastwave, since the n_p, T, U profiles bear no resemblance to those computed for blast waves (Figure 6). Although the energy ($\sim 6 \times 10^{31}$ ergs) and mass ($\sim 2 \times 10^{16}$ gm) integrated over the disturbance are "intermediate", the n_p, T, U profiles differ from those computed for intermediate type

shock waves (Hundhausen, 1972). The 2-stage model is inadequate, because a calculation similar to that used above for the March 19, event shows that an elements of plasma corresponding to the stream maximum left the sun near midday on March 31, nearly 24 hours before the onset of the flare associated with the shock. One might expect that the event could be described by the synoptic model since this is based on a synthesis of observations and theoretical concepts, but this model too does not satisfactorily either explain or describe the observations of the April 3, event: there is no single tangential discontinuity which stands out, there is no single region with a large $^4He^{++}/H^+$ ratio, and there is nothing resembling a magnetic bottle.

Essential features of the April 3, event are the shock front, a stream, and a region between the stream and the shock in which n and B are enhanced, disturbed, and discontinuous.

Although we have a clear flare association, we cannot rule out the possibility that the shock was generated by the stream or that it is independent of the stream. In either case, however, the shock and stream interact, and the density and magnetic field intensity enhancements between the shock and stream have a single explanation. Material is flowing into the interaction region from both sides carrying with it a frozen field. It is compressed and heated by the shock on the forward side and it is compressed and heated by the stream on the opposite side.

An interesting consequence of the numerous discontinuities in between the shock and the stream is that there is a series of dis-

continuities in the momentum flux, which cause sudden impulses in the horizontal component of the geomagnetic field, Figure 5. For the April 3, event, there are at least 13 conspicuous discontinuities in the momentum between the time of the shock front at 2130 UT on April 3 and 0100 UT on April 5, (labeled A though L) and each of these produced within minutes a corresponding geomagnetic impulse. Note that in two cases (E E^1 and L L^1), there was an increase in nU^2 followed within minutes by a decrease, which produced a characteristic signal in the magnetogram similar to that identified by Ogilvie et al. (1968) and designated as pl^+. No discontinuities in either H or nU^2 were observed on April 5. In particular the "discontinuity" with the signature of a slow shock did not produce such a change. The discontinuities in the region between the shock and stream, however, provide a clear signature in magnetograms which allow one to differentiate between continuous and discontinuous flows.

V. Discussion

Our analyses of the flows behind two interplanetary shock shows that conventional models and classification schemes do not satisfactorily describe either of these events. Both shock fronts were followed by streams, but in one case (March 19, 1971) n_p, T, and U decrease monotomically from the shock to the stream with no discontinuities in this region, whereas in the other case, n, T, U, and B show a very complex pattern between the shock and the stream, n and B being relatively large and discontinuous.

Hundhausen et al. (1970) have suggested that continuous shock-stream flows are entirely the result of a flare, the shock being caused directly by the explosion and the stream being the result of heat from the flare (2-stage model). We find that this model cannot explain the observed small separation between the shock and stream. We are led to an alternate explanation (the compound event model) according to which the shock and stream have different origins, the shock being caused by a flare and the stream existing before the occurrence of the flare. In the compound event model, the shock and stream can be related in many ways, as illustrated in Figure 4. If the shock is produced by a flare at $\approx 20°$W and the stream at the time of the flare is near central meridian (Figure 4a) the stream will be observed to follow the shock, but part of the shock will have actually passed through the stream. If the stream originates near the east limb of the sun, one will see the shock days before the stream passes the earth (Figure 4c). The shock and stream can also arrive simultaneously (Figure 4b). If the stream originates near the flare site but is still independent of the flare, the interval between the shock arrival time and the time of the stream maximum is approximately $t_{shock} - t_{stream} \approx (\sigma_f/w_s + R/V_s) - 4R/3V_m$, where σ_f is the longitude of the flare, w_s the angular speed of the sun, R the position of the observer, V_s is the speed of the shock, V_m is the maximum speed of the stream. In this case $t_{shock} - t_{stream}$ can obviously be $<$, $>$, or $= 0$, depending on the value of $\sigma_f - Rw_s\,(4/3V_m - 1/V_s)$. Of course, we do not suggest that the compound event model applies to all shock

waves, but that it can explain certain complications in observed flows.

The discontinuous shock-stream flow is more complicated than the continuous shock-stream flow and we cannot exclude the possibility that the shock is generated by the stream itself. However, the 2-stage model can be eliminated, and if one assumes that the compound event model applies, one finds that the shock has moved through the stream. In any case, the complexity of the region between the shock front and the stream can be attributed to the interaction between the material which passed through the shock front and that which was modified by the stream.

Ogilvie and Burlaga (1969) have emphasized the complexity of post-shock flows. The two examples in this paper represent only two particular types of post-shock flow patterns. We regard the complexity of post-shock flows as fundamental and not just a matter of detail, which is unfortunate from an analytical point of view, but cannot be ignored. We suggest that this complexity can better be understood if one considers that shocks and associated streams can have different origins and can interact in many ways.

Acknowledgements

The authors thank N. F. Ness for providing the magnetic field measurements used in this study. Ness, Chao, Lepping, and Sugiura contributed valuable questions and suggestions with regard to a draft of this paper.

Figure Captions

1. The sum of magnetic and thermal energy densities $\left[B^2/8\pi + n_p\ kT_p + n_\alpha\ kT_\alpha\right]$ for the period March 18 to April 8, 1971.
2. Observations of $\frac{N_p U^3}{2}$, U, n_p, T_p, B, θ, Φ and n_α/n_p for the March 19, 1971 shock.
3. The magnitude B and two angles and for the March 19 shock at higher time resolution, showing the angular charges in the magnetic field immediately after passage of the shock.
4. This illustrates the compound event model, and shows predictions for the cases where the stream follows the shock (A), the stream occurs at the same time as the shock (B), and the shock is far ahead of the stream (C).
5. Ground magnetograms for March 19 and 20th and April 3 and 4 from the Honolulu station.
6. Observations of $\frac{N_p U^3}{2}$, U, n_p, T_p, B, θ, Φ and n_α/n_p for the 3 April 1971 event.

References

Burlaga, L. F., Anisotropic Diffusion of Solar Cosmic Rays, J. Geophys. Res., 72, 17, 1967.

Burlaga, L. F., Shock Phenomena in Interplanetary Space, NASA-X 692-72-395, 1972

Burlaga, L. F., and J. K. Chao, Reverse and forward slow shocks in the solar wind, J. Geophys. Res., 76, 7516, 1971.

Burlaga, L. F., and K. W. Ogilvie, Magnetic and Thermal Pressures in the Solar Wind, Solar Phys., 15, 61, 1970.

Chao, J. K., and R. P. Lepping, A correlative study of SSC'S interplanetary shocks, and solar activity, submitted to J. Geophys. Res., 1973.

Chao, J. K., and S. Olbert, Observation of slow shocks in interplanetary space, J. Geophys. Res., 75, 6394, 1970.

Colburn, D. S., and C. P. Sonett, Space Sci Rev., 5, 439, 1968.

Dryer, M., Interplanetary Shock Waves Generated by Solar Flares, Space Science Reviews, in press, 1973.

Gosling, J. T., J. R. Asbridge, S. J. Bame, A. J. Hundhausen, and I. B. Strong, Satellite Observations of Interplanetary Shock Waves, J. Geophys. Res., 73, 43, 1968.

Hundhausen, A. J., "Coronal Expansion and Solar Wind", Springer, 1972.

Hundhausen, A. J., and R. A. Gentry, J. Geophys. Res., 74, 2908, 1969.

Hundhausen, A. J., S. J. Bame, and M. D. Montgomery, Large-Scale Characteristics of Flare Associate, Solar Wind Disturbances, J. Geophys. Res., 75, 463, 1970.

Korobeinikov, V. P., and Yu. M. Nikolayev, Cosmic Electrodynamics, 3, 25, 1972.

Montgomery, M. D., S. W. Bame, and A. J. Hundhausen, "Solar Wind Electrons Vela 4 Measurements", J. Geophys. Res., 73, 4999, 1968.

Ogilvie, K. W., "Co-rotating shock structures", NASA SP-308, p 430, 1972.

Ogilvie, K. W., and L. F. Burlaga, "Hydromagnetic Observations of the Solar Wind," The Earth's Particles and Fields, ed., B. McCormac, Reidel, 1969.

Ogilvie, K. W., L. F. Burlaga, and T. D. Wilkerson, Plasma Observations on Explorer 34, J. Geophys. Res., 73, 6809, 1968.

Parker, E. N., Interplanetary Dynamical Processes, Interscience, New York, 1963.

Scudder, J. D., K. W. Ogilvie and D. Lind, J. Geophys. Res., in press 1973.

Unti, T, Neugebauer, M, and C. S. Wu, "Shock system of February 2 1969," J. Geophys. Res, 78, 7237, 1973.

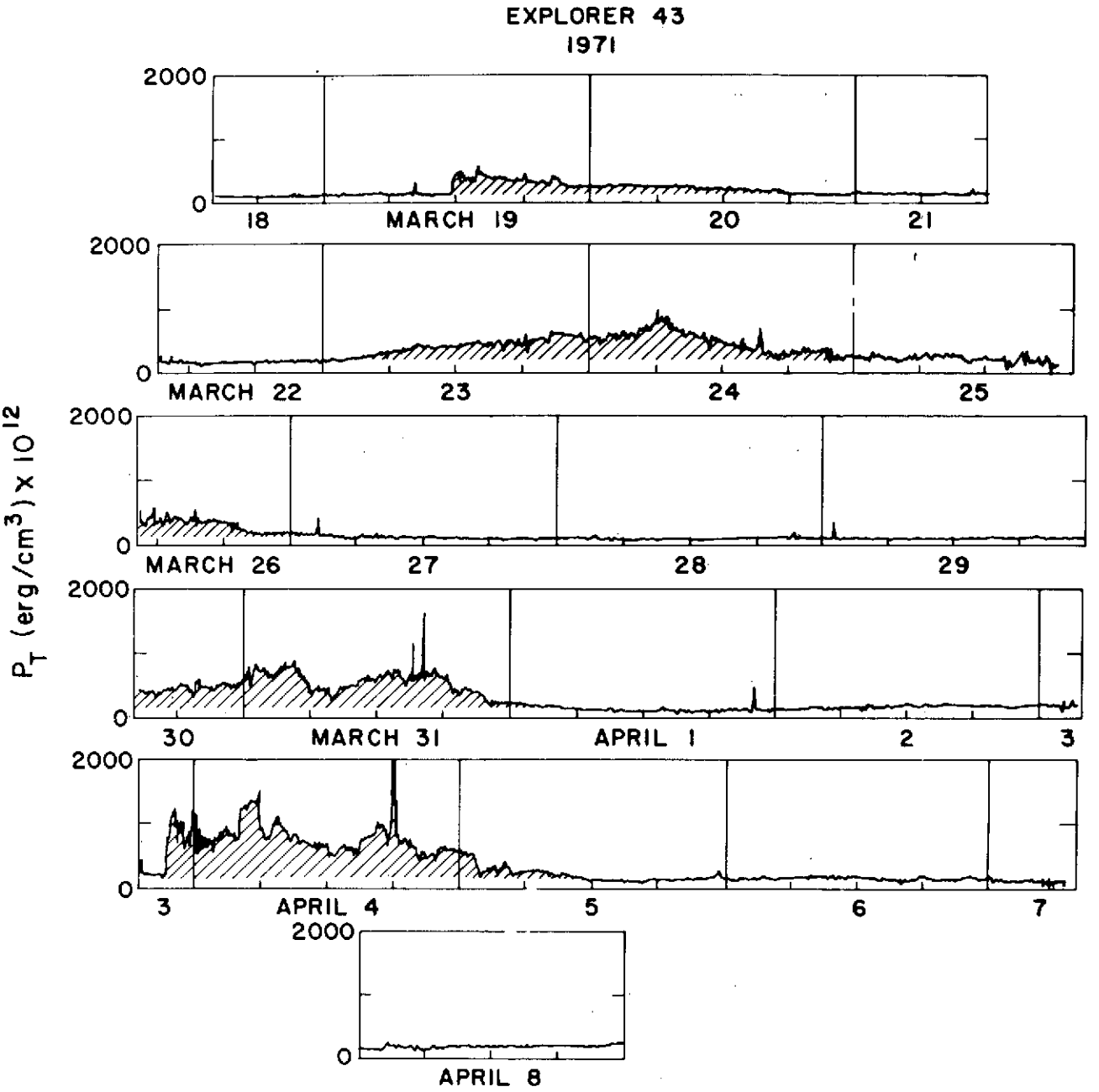
EXPLORER 43
1971
2000
0
18
MARCH 19
20
21
MARCH 22
23
24
25
MARCH 26
27
28
29
30
MARCH 31
APRIL 1
2
3
APRIL 4
5
6
7
APRIL 8
P_T (erg/cm^3) X 10^{12}

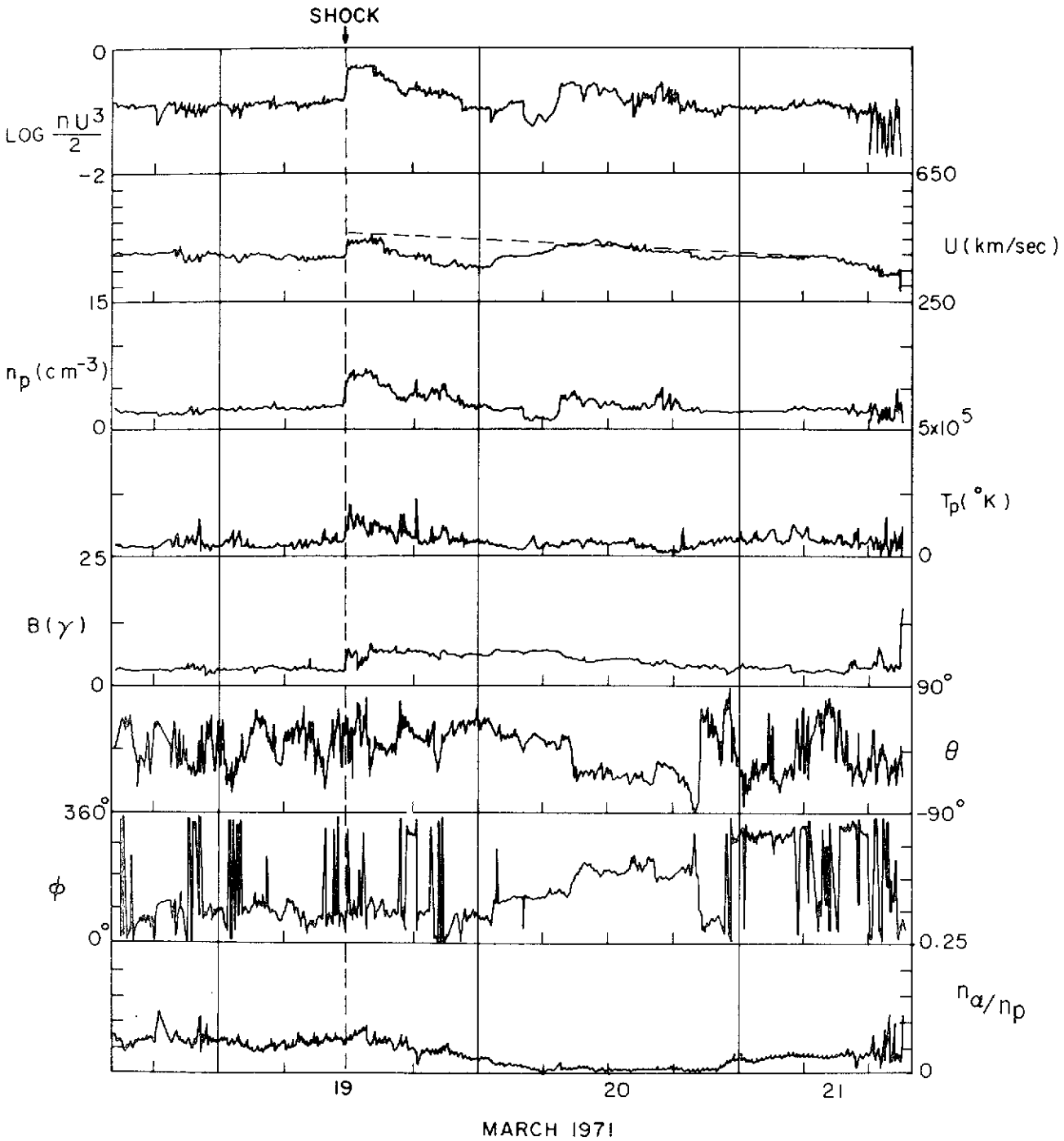
SHOCK
0
LOG nU³/2
-2
650
U (km/sec)
15
250
n_p (cm⁻³)
0
5x10⁵
T_p (°K)
25
0
B (γ)
0
90°
θ
360°
-90°
φ
0°
0.25
n_α/n_p
0
19
20
21
MARCH 1971

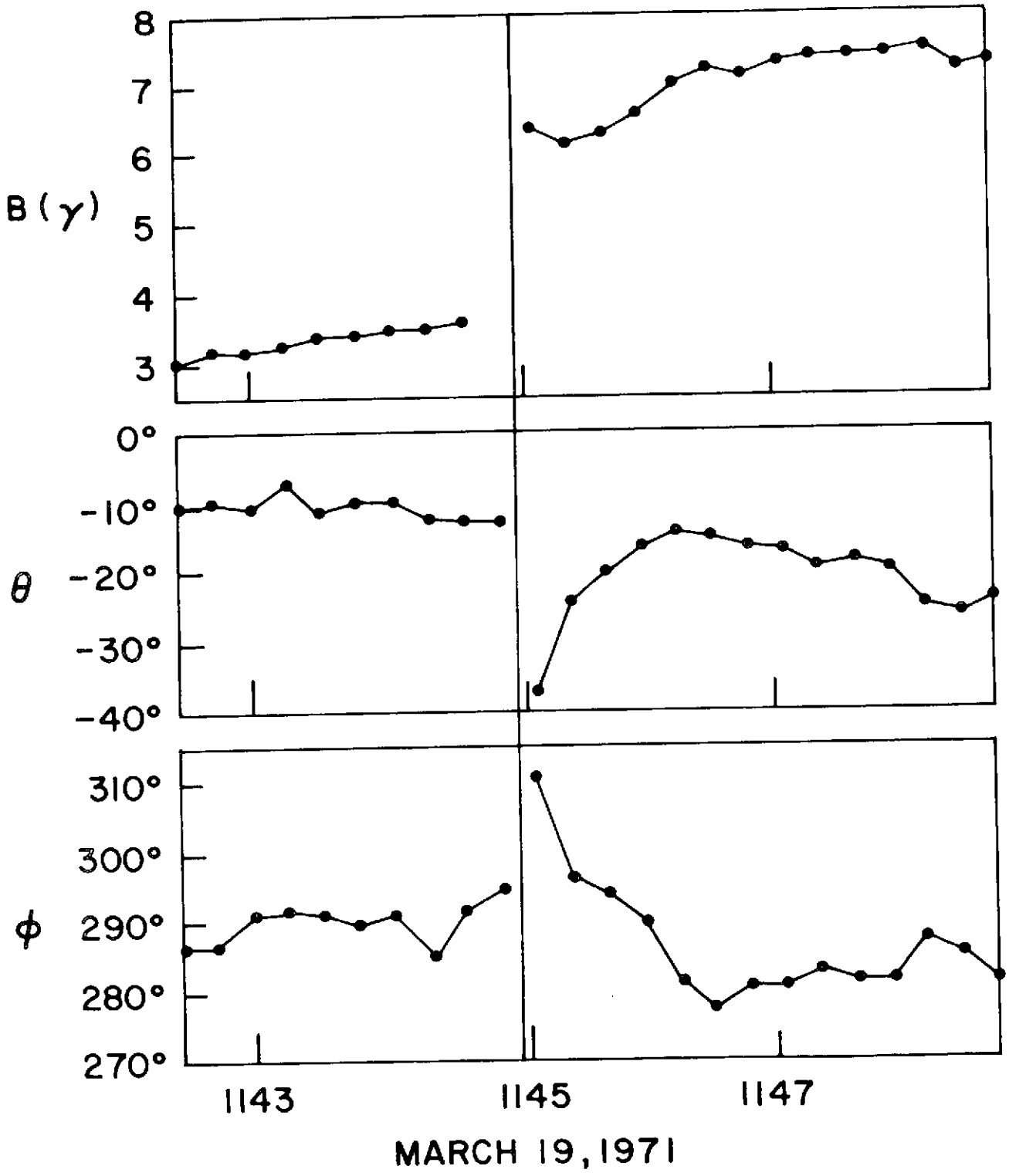
8
7
6
5
4
3
B (γ)
0°
-10°
-20°
-30°
-40°
θ
310°
300°
290°
280°
270°
φ
1143
1145
1147
MARCH 19, 1971

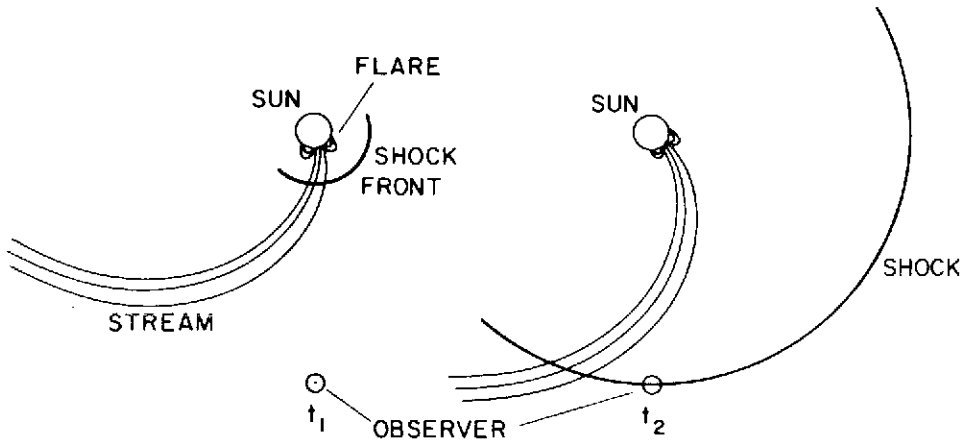

A. STREAM FOLLOWS SHOCK

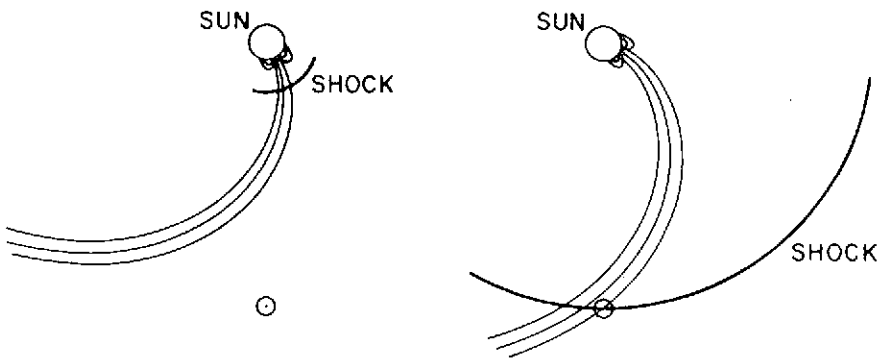

B. STREAM AND SHOCK SIMULTANEOUS

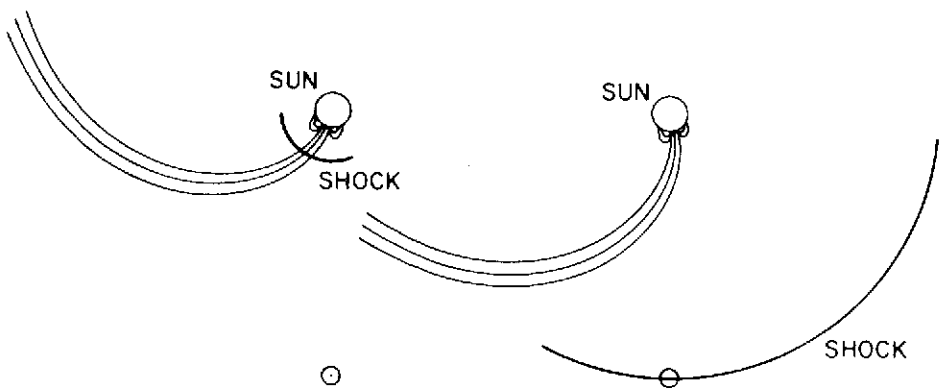

C. SHOCK FAR AHEAD OF STREAM

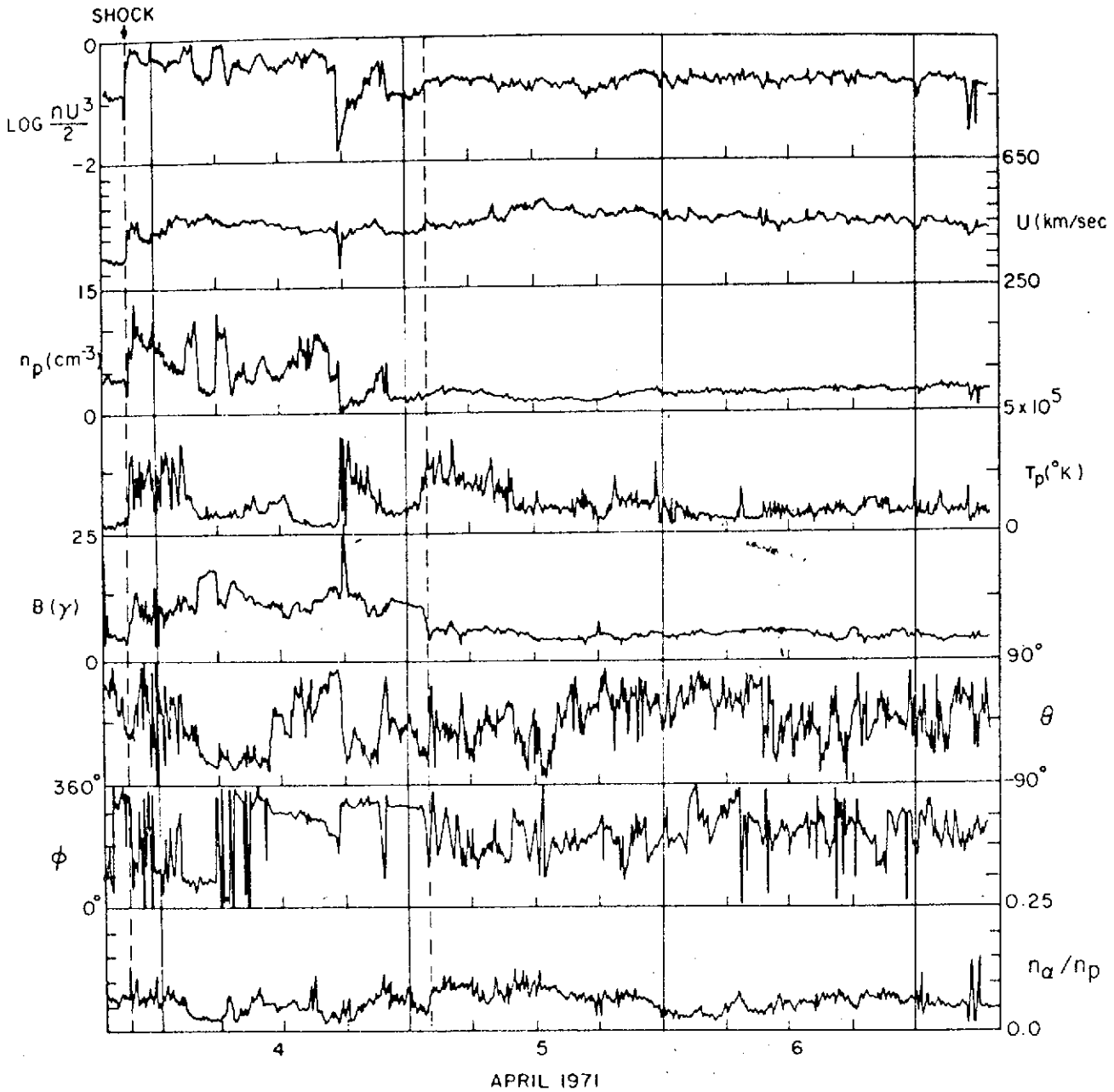
SHOCK
LOG $\frac{nU^3}{2}$
0
-2
650
U (km/sec
250
15
n_p (cm^{-3})
0
5×10^5
T_p(°K)
25
B (γ)
0
90°
θ
360°
-90°
φ
0°
0.25
n_α / n_p
0.0
4
5
6
APRIL 1971

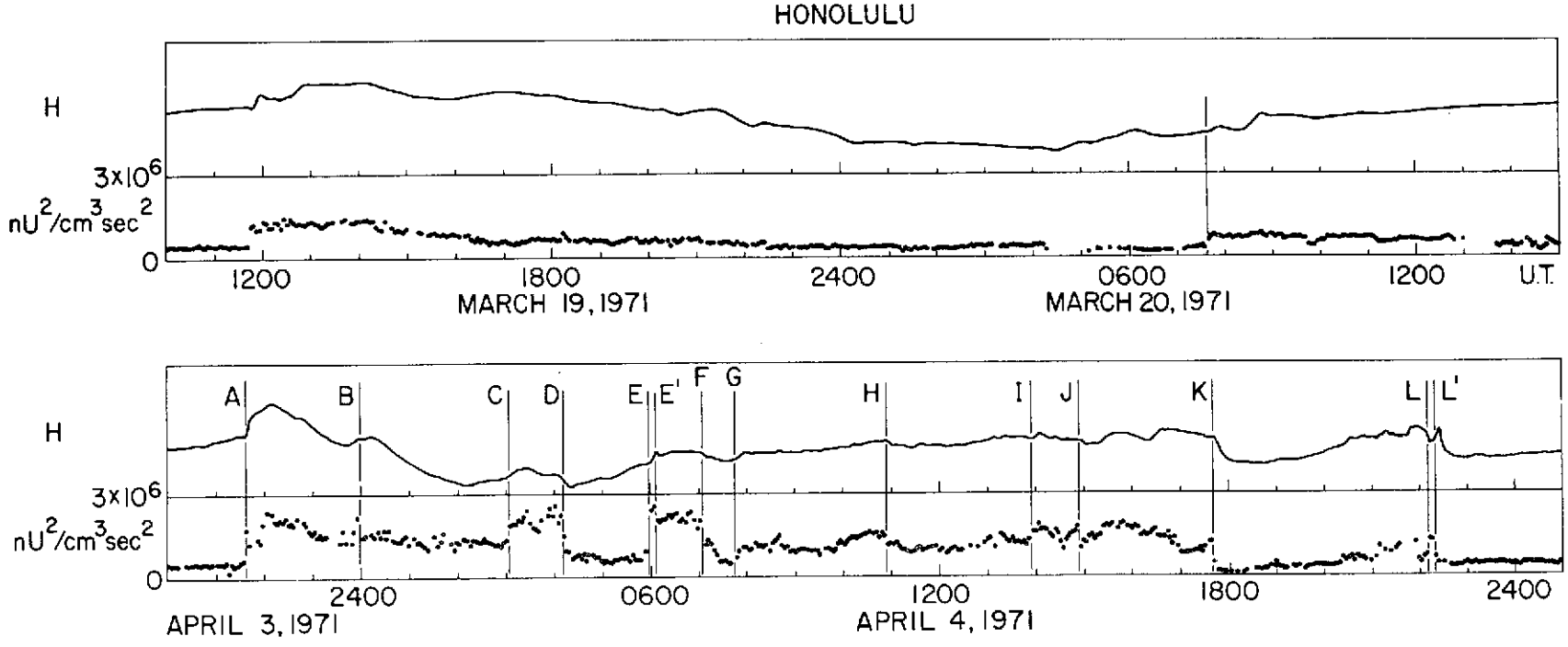
HONOLULU
H
3x10^6
nU^2/cm^3sec^2
0
1200
1800
2400
0600
1200
U.T.
MARCH 19, 1971
MARCH 20, 1971
A
B
C
D
E
E'
F
G
H
I
J
K
L
L'
H
3x10^6
nU^2/cm^3sec^2
0
2400
0600
1200
1800
2400
APRIL 3, 1971
APRIL 4, 1971